arXiv:1410.8454v2 [quant-ph] 18 Nov 2014

Knowing "where the photons have been"

Karol Bartkiewicz,[1,2,*] Antonín Černoch,[2,†] Dalibor Javůrek,[2] Karel Lemr,[2,‡] Jan Soubusta,[3] and Jiří Svozilík[2]

[1] *Faculty of Physics, Adam Mickiewicz University, PL-61-614 Poznań, Poland*
[2] *RCPTM, Joint Laboratory of Optics of Palacký University and Institute of Physics of Academy of Sciences of the Czech Republic, 17. listopadu 12, 771 46 Olomouc, Czech Republic*
[3] *Institute of Physics of Academy of Sciences of the Czech Republic, Joint Laboratory of Optics of PU and IP AS CR, 17. listopadu 50A, 772 07 Olomouc, Czech Republic*

(Dated: November 19, 2014)

Linear-optical interferometers play a key role in designing circuits for quantum information processing and quantum communications. Even though nested Mach-Zehnder interferometers appear easy to describe, there are occasions when they provide unintuitive results. This paper explains the results of a highly discussed experiment performed by Danan *et al.* [Phys. Rev. Lett. **111**, 240402 (2013)] using a standard approach. We provide a simple and intuitive one-state vector formalism capable of interpreting their experiment. Additionally, we cross-checked our model with a classical-physics based approach and found that both models are in complete agreement. We argue that the quantity used in the mentioned experiment is not a suitable which-path witness producing seemingly contra-intuitive results. To circumvent this issue, we establish a more reliable which-path witness and show that it yields well expected outcomes of the experiment.

PACS numbers: 42.50.-p, 42.50.Dv, 42.50.Ex

In quantum mechanics (QM) particles are assigned a wave function used to describe their properties [1]. This approach sometimes leads to conclusions about experimental results that seem to contradict intuitive estimations based on classical physics [2, 3]. Despite this flaw, QM is currently widely accepted as a theory [1, 4], that makes accurate predictions in agreement with the performed experiments. Therefore, it is considered valid regularly used for the interpretation of the results of the corresponding experiments.

Recently, an experiment that contained counter-intuitive features was proposed and realized by Danan *et al.* [5]. The authors used nested Mach-Zehnder interferometers (MZI), shown in Fig. 1, and mirrors (A, B, C, E, F) vibrating with different frequencies, in order to leave a mark on passing photons. At one selected output port of the interferometer, the photons were detected by a quad-cell detector D capable of tracing the spatial vibrations of the photon beam. After measurement, the collected signal was further processed and subjected to the Fourier transform. From the obtained frequencies of vibrations, the authors judged whether the detected photons have interacted with the mirror that was oscillating at this particular frequency.

The results described in the article by Danan *et al.* [5] were interpreted by means of two-state vector formalism (TSVF) and weak values. Both the results and their unusual interpretation were questioned [6–10]. The critical comments pertained to the visibility of interference inside the interferometer, the correct application of TSVF, the processing of the obtained data and its validity. Until now, no-one has managed to provide the theoretical calculations and the interpretation of the experimental results using only the standard one-state vec-

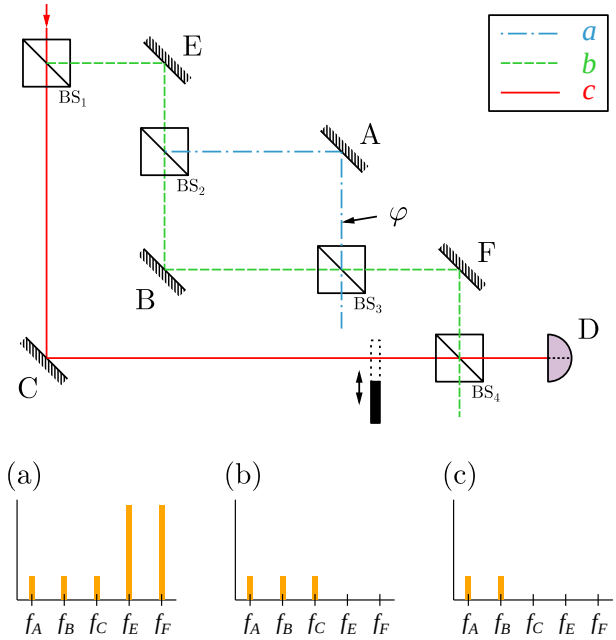

FIG. 1: (Color online) Drawing of the experimental setup with two nested Mach-Zender interferometers. (a) Power spectrum on detector D shows all frequencies of mirror oscillations for the phase $\varphi = \pi$, (b) power spectra for $\varphi = 0$, (c) power spectrum for phase $\varphi = 0$ and the lower path $\hat{c}$ blocked as predicted by our approach.

*Electronic address: bark@amu.edu.pl
†Electronic address: antonin.cernoch@upol.cz
‡Electronic address: k.lemr@upol.cz

tor quantum-mechanical approach. Assuming the above-mentioned approach makes it possible to interpret the results from Ref. [5] and verify their congruity with QM. Consequently, we would manage to shed more light on the ongoing discussion regarding the legitimacy of the experimental data and its interpretation. In our opinion, this would be useful for describing experiments similar to [5] clarifying the debate about the experiment.

In this paper, we present a relevant standard one-state vector formalism and describe the evolution of the state vector as it passes the MZI in the direction of the detector. We describe the post selection process and derive the probabilities of detecting at particular frequencies (that correspond to the vibrations of the individual mirrors). The obtained results are compared with the experimental data presented by Danan *et al.* [5]. Finally, we use classical optics to describe the transverse profiles of the light beams used in the experiment and we apply the result to validate the one-state vector outcomes at the classical limit.

A correct description of Danan *et al.* experiment needs to consider all the photon modes present in the setup. Apart from the spatial modes, additional modes are introduced by vibrations of the mirrors (referred as the "frequency modes"). The modes must be taken into account, since they differentiate, at least in principle, between the respective paths of the photon. Our analysis uses the formalism of annihilation operators and their transformations on beam splitters (BS). Spatial modes are labeled by operators $\hat{a}$, $\hat{b}$ and $\hat{c}$, while the frequency modes are marked by binary numbers. The five frequency modes are introduced by the mirrors A, B, C, E or F. They are marked by consecutive binary indices after the symbol naming the spatial mode. The index value is either 0 or 1, indicating whether mode frequency was modulated by a corresponding mirror (1) or not (0). So, for instance, if spatial mode $\hat{a}$ was frequency modulated by mirrors A, E and F, it would be indexed as $\hat{a}_{10011}$.

At the beginning the photon is in the mode $\hat{c}_{00000}$ (see setup depicted in Fig. 1). The first beam-splitter (BS_1) divides the beam with an intensity ratio of 1:2. As a result, the spatial mode gets transformed to

$$\hat{c}_{00000} \to \frac{1}{\sqrt{3}}\hat{c}_{00000} + \sqrt{\frac{2}{3}}\mathrm{i}\hat{b}_{00000}. \quad (1)$$

In the outer arm, the spatial mode $\hat{c}$ interacts with the vibrating mirror C, while the reflected mode $\hat{b}$ comes into contact with the mirror E. This is described by transition

$$\frac{1}{\sqrt{3}}\hat{c}_{00000} + \sqrt{\frac{2}{3}}\mathrm{i}\hat{b}_{00000} \to \frac{1}{\sqrt{3}}\hat{c}_{00100} + \sqrt{\frac{2}{3}}\mathrm{i}\hat{b}_{00010}. \quad (2)$$

The spatial mode $\hat{b}$ now enters the inner interferometer formed by two balanced beam splitters. The first beam splitter, BS_2, transforms it to

$$\hat{b}_{00010} \to \frac{1}{\sqrt{2}}\hat{b}_{00010} + \frac{1}{\sqrt{2}}i\hat{a}_{00010}. \quad (3)$$

The vibrating mirrors A and B then have the following effect

$$\frac{1}{\sqrt{2}}\left(\hat{b}_{00010} + i\hat{a}_{00010}\right) \to \frac{1}{\sqrt{2}}\left(\hat{b}_{01010} + i\hat{a}_{10010}\right). \quad (4)$$

The difference between the lengths of the upper and lower arms of the inner interferometer introduces an additional phase shift that can be attributed solely to the mode $\hat{a}$

$$\hat{a}_{10010} \to \mathrm{e}^{\mathrm{i}\varphi}\hat{a}_{10010}. \quad (5)$$

The modes $\hat{b}$ and $\hat{a}$ get recombined on the second beam splitter of the inner interferometer, i.e., BS_3. At this point we disregard the outgoing mode $\hat{a}$ since only the mode $\hat{b}$ can further contribute to photon detection, hence

$$\frac{1}{\sqrt{2}}\left(\hat{b}_{01010} + \mathrm{i}\mathrm{e}^{\mathrm{i}\varphi}\hat{a}_{10010}\right) \to \frac{1}{2}\left(\hat{b}_{01010} - \mathrm{e}^{\mathrm{i}\varphi}\hat{b}_{10010}\right). \quad (6)$$

The output mode of the inner interferometer, $\hat{b}$, meets the last vibrating mirror, F,

$$\frac{1}{2}\left(\hat{b}_{01010} - \mathrm{e}^{\mathrm{i}\varphi}\hat{b}_{10010}\right) \to \frac{1}{2}\left(\hat{b}_{01011} - \mathrm{e}^{\mathrm{i}\varphi}\hat{b}_{10011}\right). \quad (7)$$

Finally, we recombine the modes $\hat{c}$ and $\hat{b}$ on the last unbalanced beam splitter BS_4 (identical to BS_1). The final form of the spatial mode $\hat{c}$, describing photons that reach detector D, is

$$\frac{1}{3}\left(\hat{c}_{00100} - \hat{c}_{01011} + \mathrm{e}^{\mathrm{i}\varphi}\hat{c}_{10011}\right). \quad (8)$$

As in the case of the inner interferometer, we discard the output mode $\hat{b}$ that can not lead to photon detection at the detector D. We assume that the photons entering this setup are single photons that can be described in therm of the creation operator $\hat{a}^\dagger|0\rangle$. The output state in the Fock basis then reads

$$\begin{aligned} |\psi_{\mathrm{out}}\rangle &= \frac{1}{3}\left(\hat{a}^\dagger_{00100} - \hat{a}^\dagger_{01011} + \mathrm{e}^{\mathrm{i}\varphi}\hat{a}^\dagger_{10011}\right)|0\rangle \\ &= \frac{1}{3}\left(|1\rangle_{00100} - |1\rangle_{01011} + \mathrm{e}^{\mathrm{i}\varphi}|1\rangle_{10011}\right). \end{aligned} \quad (9)$$

We use the same labeling for the annihilation operators and frequency modes. Note that the authors of the experiment [5] set the phase shift in the inner interferometer to $\varphi = 0$, π [see Fig.2 in Ref. [5]].

To explain the results of [5], it is crucial to correctly describe the post-selection process caused by photon detection and subsequent frequency mode analysis. When one particular frequency mode is post-selected, the information about the photon being in a superposition of other frequency modes is erased. The frequency modes are orthogonal, i.e., one can perform a direct deterministic signal frequency analysis to distinguish between the modes [11]. Thus, post-selecting a specific frequency mode makes the information about the other frequency modes unavailable.

Post-selection is a well established technique in quantum state engineering used, e.g., in optimal quantum cloning [12]. Here, the post-selection on the photon that interacted with mirror A is formally equivalent to the projection of the output state onto the state

$$|\Pi_A\rangle = \sum_{A,B,C,E,F=0,1} \delta_{A,1}|1\rangle_{ABCEF}, \tag{10}$$

where $\delta_{A,1}$ is Kronecker's delta. Post-selection on any other mode is also defined by Eq (10), where A in Kronecker's delta is replaced with a chosen mode, i.e., $A \leftrightarrow X$ for $X = B$, C, E, F. Now, one can immediately see from Eq. (9) that

$$|\langle\Pi_A|\psi_{\rm out}\rangle|^2 = \frac{1}{9} \tag{11}$$

and, similarly,

$$|\langle\Pi_B|\psi_{\rm out}\rangle|^2 = |\langle\Pi_C|\psi_{\rm out}\rangle|^2 = \frac{1}{9}. \tag{12}$$

The structure of the output state implies that post-selecting modes E and F yields the same results for both. For mode E one obtains

$$\begin{aligned}\langle\Pi_E|\psi_{\rm out}\rangle &= \frac{1}{3}\left(-\langle\Pi_E|1\rangle_{01011} + {\rm e}^{{\rm i}\varphi}\langle\Pi_E|1\rangle_{10011}\right)\\ &= \frac{2}{3}{\rm e}^{{\rm i}\varphi/2}\sin\varphi = \langle\Pi_F|\psi_{\rm out}\rangle.\end{aligned} \tag{13}$$

Thus, for $\varphi = 0$ none of the frequency modes marked as E or F will contribute to the final state. If the phase shift is set to $\varphi = \pi$, both modes will appear as $|\langle\Pi_E|\psi_{\rm out}\rangle|^2 = |\langle\Pi_F|\psi_{\rm out}\rangle|^2 = \frac{4}{9}$.

Let us use the theoretical framework established above to explain the experimental data in Ref. [5]. In case of constructive interference [$\varphi = \pi$, see Fig. 1(a)], all frequencies f_X for $X = A$, B, C, E, F are present in the power spectrum recorded by detector D. Intensities for frequencies f_E and f_F are four times higher than others because of constructive interference in the inner MZI. Destructive interference appears for $\varphi = 0$ [see Fig. 1(b)] and it removes the peaks for frequencies f_E and f_F from the power spectrum. The peaks for frequencies f_A and f_B remain constant because post-selecting on mode A or B is equivalent to post-selecting on a photon traveling via the post-selected arm of the inner MZI, so there is no interference at the BS_3.

The experimental results presented in Figs. 2(a) and 2(b) of Ref. [5] agree with our theoretical predictions. If the photon reflected from mirror C is blocked and the phase shift is $\varphi = 0$ [see Fig. 1(c)], our theoretical prediction does not match the experimental data from Ref. [5]. In this case we predict that f_A, f_B should be constant (similarly to the previously discussed cases). This is because it is possible to distinguish between photons reflected from mirrors A and B. When mode post-selection (power spectrum analysis) is performed the interference on BS_3 is effectively removed. Therefore, it should be possible to observe the intensity peaks for f_A and f_B. As we present below, the intensity peaks for f_A and f_B are also predicted by the classical theory of light.

The classical approach to deriving frequency-mode amplitudes is based on the standard electromagnetic-wave theory (Supplemental Material of Ref. [5]). We repeated this classical procedure, but we did not keep track of the normalization factors and took only those parts of the expressions that were relevant. The amplitude of the electric field at the detector D takes in general the form of

$$\begin{aligned}\Psi(y,t) \;\propto\; &\kappa{\rm e}^{-(y-d_C)^2} - {\rm e}^{-(y-d_A-d_E-d_F)^2}\\ &+{\rm e}^{{\rm i}\varphi}{\rm e}^{-(y-d_B-d_E-d_F)^2},\end{aligned}$$

where $\kappa = 1$ ($\kappa = 0$) when mode c is open (closed) and d_X are small shifts in direction y oscillating with frequencies of the relevant mirror labeled with $X = A, B, C, E, F$. The amplitude expressed using the paraxial approximation reads

$$\begin{aligned}\Psi(y,t) \;\propto\; &{\rm e}^{-y^2}\left[\kappa - 1 + {\rm e}^{{\rm i}\varphi} + 2\kappa y d_C - 2y d_A + {\rm e}^{{\rm i}\varphi}2y d_B\right.\\ &\left.+2y\left({\rm e}^{{\rm i}\varphi} - 1\right)(d_E + d_F)\right]\end{aligned} \tag{14}$$

Let us use Eq. (14) to calculate the intensities in all three scenarios shown in Fig. 2 of [5]. In the first scenario (a) there is constructive interference in the small MZI and mode c is open, i.e., we set $\kappa = 1$ and $\varphi = \pi$. The associated field amplitude reads

$$\Psi_{\rm a}(y,t) \;\propto\; {\rm e}^{-y^2}\left[1 + 2y\left(d_A + d_B - d_C + 2d_E + 2d_F\right)\right] \tag{15}$$

The measurement performed by Danan *et al.* [5] consists of evaluating the power spectrum of the function

$$\Delta I_a(t) \equiv \int_0^\infty |\Psi_a(y,t)|^2{\rm d}y - \int_{-\infty}^0 |\Psi_a(y,t)|^2{\rm d}y. \tag{16}$$

The Fourier transform of $\Delta I_a(t)$ is $\Delta I_a(f) \propto \delta(f - f_A) + \delta(f - f_B) + \delta(f - f_C) + 2\delta(f - f_E) + 2\delta(f - f_F)$. It provides five peaks in the associated power spectrum $|\Delta I_a(f)|^2$, where peaks corresponding to frequencies f_A, f_B, f_C have four times smaller area than peaks for f_E, f_F. Note that the corresponding intensity difference ratios are 1:2 (in contrast to our quantum model, which describes a sum of intensities).

In the second scenario (b) mode c is open ($\kappa = 1$) and there is destructive interference in the small MZI ($\varphi = 0$). Thus, the field amplitude

$$\Psi_b(y,t) \;\propto\; {\rm e}^{-y^2}\left[1 + 2y\left(d_C - d_A + d_B\right)\right] \tag{17}$$

provides the power spectrum of $|\Delta I_a(f)|^2$ containing three balanced peaks associated with mirrors A, B and C (the same result is provided by our quantum model).

In the third scenario (c), the mode c is blocked ($\kappa = 0$) and $\varphi = 0$. The amplitude

$$\Psi_c(y,t) \;\propto\; 2y{\rm e}^{-y^2}\left(d_A - d_B\right) \tag{18}$$

in this case provides intensity $|\Psi_c(y,t)|^2$ that is even function of y, hence $\Delta I_c = 0$. Therefore, no peaks are observed by Danan *et al.* [5]. On the other hand, it follows from Eq. (18) that the amplitude and the resulting intensity oscillates with frequencies f_A and f_B. It means that these quantities include the information about the photons impinging on the mirrors A and B. However, the specific quantity measured by Danan *et al.* [5] ignores this information. This leads us to conclude that ΔI is not a reliable which-path witness because it ignores some of the available information.

In order to use the available information to its fullest extent we propose to use spectrum of the overall intensity

$$I_T(f) \equiv \int_{-\infty}^{\infty} |\Psi(y,f)|^2 \mathrm{d}y$$

where $\Psi(y,f)$ is a Fourier transform of the field $\Psi(y,t)$ (the parameters of which can be established from the setup configuration and $I(t)$ measurements). This quantity is a more reliable which-path witness and it corresponds to our quantum model. Note that I_T does not vanish for even $|\Psi(y,f)|^2$ (in contrast to ΔI). The total intensity $I_T(f)$ contains contributions from the respective mirror frequencies. The weights associated with the specific mirrors can be calculated as $w(f_X) = I_T(f_X)\,\mathrm{d}f,$, where f_X stands for the respective mirrors frequencies. This approach produces exactly the same results as obtained by the previously mentioned quantum approach. In scenario (a), the intensity $I_T(f)$ provides the weights $w(f_X)$ of the five peaks that have the 1:4 ratio. In scenario (c) $I_T(f)$ does not hide the which-path information encoded in the presence of frequency peaks corresponding to mirrors A and B (see Fig. 1).

In this paper, we described the spectra at the output port of nested MZI with vibrating mirrors applying both quantum and classical theories of light. The quantum approach employed the standard formalism of annihilation operators and one-state vectors in Fock's basis. The time-dependent transverse profiles of beams were described classically and used in the analysis of the spectrum of the electric field. Using the classical approach, we have explained the results observed by Danan *et al.* [5] and established that the quantity they used is not a reliable which-path witness. We, therefore, propose to acquire spectrum of the overall intensity instead and show that it produces well expected results that can be described both classically and in a quantum way.

Acknowledgements

The authors thank Jára Cimrman for his helpful suggestions and David Schmid for a very fruitful discussion. K. L. acknowledges support by the Czech Science Foundation (Grant No. 13-31000P). D. J. acknowledges support by project IGA_PrF_2014005 of IGA UP Olomouc. K. B. acknowledges support by the Foundation for Polish Science and the Polish National Science Centre under grant No. DEC-2013/11/D/ST2/02638. Finally, the authors acknowledge the project No. LO1305 of the Ministry of Education, Youth and Sports of the Czech Republic.

[1] M. S. R. P. Feynamn, R. B. Leighton, *The Feynman Lectures on Physics, Vol. III: The New Millennium Edition: Quantum Mechanics (Volume 2)* (Basic Books; First Trade Paper Edition edition, 2011), 2nd ed.
[2] N. R. A. Einstein, B. Podolsky, Physical Review **47**, 777 (1935).
[3] G. Blaylock, American Journal of Physics **78**, 111 (2010).
[4] M. Jammer, *The conceptual development of quantum mechanics* (McGraw-Hill, 1966), 1st ed.
[5] A. Danan, D. Farfurnik, S. Bar-Ad, and L. Vaidman, Physical Review Letters **111**, 240402 (2013), ISSN 0031-9007.
[6] M. Wieśniak, arXiv:1407.1739v1 (2014).
[7] H. Salih, arXiv:1401.4888v2 (2014).
[8] B. E. Y. Svensson, arXiv:1402.4315v2 (2014).
[9] J. Huang, L. Hu, X. Xu, C. Liu, Q. Guo, H. Zhang, and S. Zhu, arXiv:1402.4581v1 (2014).
[10] F. Li, F. A. Hashmi, J.-X. Zhang, S.-Y. Zhu, arXiv:1410.7482 (2014).
[11] S. M. Barnett and S. Croke, Advances in Optics and Photonics **1**, pp. 238–278 (2009).
[12] K. Bartkiewicz, A. Černoch, K. Lemr, J. Soubusta, M. Stobińska, Phys. Rev. A **89**, 062322 (2014); K. Bartkiewicz, K. Lemr, A. Černoch, J. Soubusta, A. Miranowicz, Phys. Rev. Lett. **110**, 173601 (2013); K. Lemr, K. Bartkiewicz, A. Černoch, J. Soubusta, A. Miranowicz, Phys. Rev. A **85**, 050307(R), (2012).